



OPEN ACCESS

EDITED BY

Krista DiSano,
White River Junction VA Medical Center,
United States

REVIEWED BY

Danijela Savic,
University of Belgrade, Serbia
Pablo Bascañana,
San Carlos University Clinical Hospital, Spain

*CORRESPONDENCE

Sini Laaksonen
✉ sjkorp@utu.fi

RECEIVED 07 December 2023

ACCEPTED 31 January 2024

PUBLISHED 20 February 2024

CITATION

Laaksonen S, Saraste M, Nylund M, Hinz R, Snellman A, Rinne J, Matilainen M and Airas L (2024) Sex-driven variability in TSPO-expressing microglia in MS patients and healthy individuals.
Front. Neurol. 15:1352116.
doi: 10.3389/fneur.2024.1352116

COPYRIGHT

© 2024 Laaksonen, Saraste, Nylund, Hinz, Snellman, Rinne, Matilainen and Airas. This is an open-access article distributed under the terms of the [Creative Commons Attribution License \(CC BY\)](https://creativecommons.org/licenses/by/4.0/). The use, distribution or reproduction in other forums is permitted, provided the original author(s) and the copyright owner(s) are credited and that the original publication in this journal is cited, in accordance with accepted academic practice. No use, distribution or reproduction is permitted which does not comply with these terms.

Sex-driven variability in TSPO-expressing microglia in MS patients and healthy individuals

Sini Laaksonen^{1,2,3*}, Maija Saraste^{1,3}, Marjo Nylund^{1,2,3,4},
Rainer Hinz⁵, Anniina Snellman^{1,3}, Juha Rinne^{1,2,3,4},
Markus Matilainen^{1,3} and Laura Airas^{1,2,3,4}

¹Turku PET Centre, Turku University Hospital, University of Turku, Turku, Finland, ²Neurocenter, Turku University Hospital, Turku, Finland, ³Clinical Neurosciences, University of Turku, Turku, Finland, ⁴InFLAMES Research Flagship, University of Turku, Turku, Finland, ⁵Wolfson Molecular Imaging Centre, University of Manchester, Manchester, United Kingdom

Background: Males with multiple sclerosis (MS) have a higher risk for disability progression than females, but the reasons for this are unclear.

Objective: We hypothesized that potential differences in TSPO-expressing microglia between female and male MS patients could contribute to sex differences in clinical disease progression.

Methods: The study cohort consisted of 102 MS patients (mean (SD) age 45.3 (9.7) years, median (IQR) disease duration 12.1 (7.0–17.2) years, 72% females, 74% relapsing–remitting MS) and 76 age- and sex-matched healthy controls. TSPO-expressing microglia were measured using the TSPO-binding radioligand [¹¹C] (R)-PK11195 and brain positron emission tomography (PET). TSPO-binding was quantified as distribution volume ratio (DVR) in normal-appearing white matter (NAWM), thalamus, whole brain and cortical gray matter (cGM).

Results: Male MS patients had higher DVRs compared to female patients in the whole brain [1.22 (0.04) vs. 1.20 (0.02), $p = 0.002$], NAWM [1.24 (0.06) vs. 1.21 (0.05), $p = 0.006$], thalamus [1.37 (0.08) vs. 1.32 (0.02), $p = 0.008$] and cGM [1.25 (0.04) vs. 1.23 (0.04), $p = 0.028$]. Similarly, healthy men had higher DVRs compared to healthy women except for cGM. Of the studied subgroups, secondary progressive male MS patients had the highest DVRs in all regions, while female controls had the lowest DVRs.

Conclusion: We observed higher TSPO-binding in males compared to females among people with MS and in healthy individuals. This sex-driven inherent variability in TSPO-expressing microglia may predispose male MS patients to greater likelihood of disease progression.

KEYWORDS

multiple sclerosis, microglia, sex, positron emission tomography, TSPO (18 kDa translocator protein)

1 Introduction

Multiple sclerosis (MS) is an autoimmune disease affecting the central nervous system (CNS). It is more common among women, with a female-to-male incidence ratio of 2.5 (1). MS is characterized by focal inflammatory lesions in white and gray matter, which leads to passing neurological symptoms, or relapses. Simultaneously with the focal inflammatory

activity, which is driven by the adaptive peripheral immune system, a neurodegenerative process commences and leads to progressive, steadily worsening symptoms. Although this smoldering process can be already present in early MS, its clinical consequences become more evident later in the disease, with increasing patient age (2).

Microglia are the principal cells of the innate immune system within the CNS, and they function as gatekeepers under normal circumstances. They defend the brain against foreign intruders and clean debris from damaged cells and synapses to ensure optimal functioning of the nervous system. Microglia receive an activation signal upon detection of foreign antigens or damaged cells and alter their function and phenotype according to the trigger (3). The functional adjustments promote re-organization of the cells within the CNS tissue, leading to increased density of microglial cells at sites of tissue damage (3, 4). The term “microglial activation” encompasses many different microglial phenotypes, both pro- and anti-inflammatory, and with numerous different functions (5). Under pathological conditions, such as in the context of neurodegeneration, microglia acquire a pro-inflammatory phenotype, which may accelerate the neurodegenerative process. This is a common phenomenon in several neurodegenerative diseases including MS (6). Neuropathological studies have demonstrated increased microglial activation characterized by pro-inflammatory marker CD68 and decreased number of homeostatic microglia in the normal-appearing white matter (NAWM) of postmortem MS brain (7).

In vivo, microglia can be assessed using positron emission tomography (PET) imaging and radioligands binding to 18kDa translocator protein (TSPO) (8–10). TSPO is a mitochondrial protein expressed by activated microglia/macrophages and reactive astrocytes and upregulated in neuroinflammation (8, 11). Although immunohistochemical studies have suggested that the upregulation of TSPO in neuroinflammation is mainly due to increased density of microglia (4, 11, 12), a recent re-analysis of three single-nucleus RNAseq studies (13–15) demonstrated increased TSPO expression in activated microglia with a pro-inflammatory phenotype (16). Regardless the fundamental reason of increased TSPO-PET signal in MS brain, clinical TSPO-PET studies have provided substantial evidence of its detrimental nature (17). Widespread, increased TSPO-binding was demonstrated in secondary progressive (SP) MS compared to relapsing–remitting (RR) MS and healthy controls (HC) (18). Increased TSPO-binding correlated well with brain atrophy measures, signs of microstructural and neuroaxonal damage, and with Expanded Disability Status Scale (EDSS) values (18–20). Moreover,

increased TSPO-binding in the NAWM and in thalamus predicted later disease worsening (18–22).

Even though women are more susceptible to develop MS, men have a higher risk of long-term disability progression. Male sex predicts a shorter time to SPMS at a younger age, and male MS patients accumulate disability faster (23, 24). Furthermore, male MS patients have imaging evidence of neurodegeneration, supported by faster brain atrophy and a higher likelihood of development of chronic hypointense T1 lesions in brain MRI (25). Furthermore, male MS patients have more severe cognitive decline than that experienced by female patients (26, 27). However, mechanisms behind these sex differences in cognition, disease progression and brain MRI findings are not well understood.

Given the convincing role of microglial activation in promoting disease progression in MS, we hypothesized that sex differences in TSPO-expressing microglia could be accelerating the more rapid disease progression experienced by men with MS. This was studied using TSPO-PET imaging in a large cohort of MS patients and healthy volunteers, with the discovery that TSPO-binding was significantly higher in males compared to females in several regions of interest (ROI) in the brain, both in MS patients and in healthy individuals.

2 Materials and methods

2.1 Study participants and study procedures

Hundred and two MS patients were recruited between 2009 and 2022 from the outpatient clinic of the Neurocenter at Turku University Hospital in Turku, Finland. They were imaged at the Turku PET Centre (TPC) using TSPO-PET and MRI. The inclusion criteria for the study were a diagnosis of MS according to diagnostic criteria appropriate to the period of diagnosis and willingness to participate in a PET study. Exclusion criteria included clinical relapse and/or corticosteroid treatment within 30 days of evaluation, gadolinium contrast enhancement in MRI, active neurological or autoimmune disease other than MS, another notable comorbidity, pregnancy and intolerance to PET or MRI. [¹¹C](R)-PK11195 data from healthy controls imaged in TPC (*n* = 37) between 2018 and 2020 or Wolfson Molecular Imaging Centre in Manchester (WMIC; *n* = 39) between 2007 and 2017 was used for comparison. Exclusion criteria for healthy volunteers were neurological or other major illness, pregnancy and intolerance to PET or MRI.

The study was conducted according to the guidelines of the Declaration of Helsinki. Study was approved by the Ethical Committee of the Hospital District of Southwest Finland and the Local Research Ethics Committee, as well as the Administration of Radioactive Substances Advisory Committee in the UK. Informed consent form was obtained from all subjects involved in the study.

PET imaging using the TSPO-radioligand [¹¹C](R)-PK11195 was performed to evaluate TSPO-expressing microglia in people with MS and HCs. For anatomic reference and the evaluation of MS pathology, MRI was obtained at the time of PET imaging. Brain MRI was performed with Philips Gyroscan Intera 1.5T Nova Dual (*n* = 25) or 3T Ingenuity TF PET/MR (*n* = 114) scanners at TPC. At WMIC, a Philips Achieva 1.5T (*n* = 25) or 3T (*n* = 14) MR scanner was used. The protocol of brain MRI for HCs included at least a 3D T1-weighted

Abbreviations: MS, multiple sclerosis; CNS, central nervous system; NAWM, normal appearing white matter; TSPO, 18kDa translocator protein; PET, positron emission tomography; SP, secondary progressive; RR, relapsing remitting; HC, healthy control; EDSS, Expanded Disability Status Scale; ROI, region of interest; TPC, Turku PET Centre; WMIC, Wolfson Molecular Imaging Centre in Manchester; FLAIR, fluid-attenuated inversion recovery; SD, standard deviation; cGM, cortical gray matter; DVR, distribution volume ratio; PF, parenchymal fraction; FDR, false discovery rate; BMI, body mass index; BP_{ND}, parametric binding potential; MNI, Montreal Neurological Institute database; FWHM, full width at half maximum; FWE, family-wise error; IQR, interquartile range; ARR, annualized relapse rate; ER, estrogen receptor; LPS, lipopolysaccharide; EAE, experimental autoimmune encephalomyelitis; TBI, traumatic brain injury.

sequence. For MS patients, a T2-weighted sequence, and a fluid-attenuated inversion recovery (FLAIR) sequence were also included for the evaluation of T2 lesions. In addition, MS patients were evaluated clinically for disability using EDSS at the time of imaging.

2.2 [¹¹C](R)-PK11195 radioligand production and PET image acquisition

The radiochemical synthesis of [¹¹C](R)-PK11195 was performed as described previously (9, 18). The mean [standard deviation (SD)] injected dose was 472 (28) MBq for MS patients and 553 (112) MBq for HCs ($p < 0.001$). In both centers, PET imaging was performed using a brain dedicated ECAT High-Resolution Research Tomograph scanner (CTI/Siemens) with an intrinsic spatial resolution of approximately 2.5 mm. A 6-min transmission scan for attenuation correction was obtained using a ¹³⁷Cs point source. After that, a 60-min dynamic emission PET scan was started simultaneously with the intravenous bolus injection of the radioligand. A thermoplastic mask was used to minimize head movements at TPC.

2.3 Creation of region of interest masks

T2- and T1-lesion ROI masks were created based on MR images performed concurrently with TSPO-PET imaging. A semi-automated method by the Lesion Segmentation Tool (28) and Carimas with manual editing slice by slice was used as described previously (18). Freesurfer 5.3 software was used to segment cortical gray matter (cGM), white matter and thalamus after the T1-lesion filling as previously reported (9). The whole brain ROI included supratentorial brain parenchyma, cerebellum, and brain stem. The NAWM ROI was created by removing the T2 lesion ROI from the WM ROI.

2.4 PET post-processing and analysis

PET images were reconstructed using 17-time frames post tracer injection, and the dynamic data were then smoothed using a Gaussian 2.5-mm post-reconstruction filter as described previously (9, 18). Possible displacements between frames due to head motion were corrected using mutual information realignment in SPM8. Finally, PET images were co-registered with the 3D T1 MRI. TSPO-expressing microglia were evaluated as specific binding of [¹¹C](R)-PK11195 using distribution volume ratio (DVR) in the prespecified ROIs: whole brain, NAWM, cGM, and thalamus. A supervised clustering technique was used to derive a clustered reference area, and ROI-level DVRs were estimated as previously described (18).

2.5 Statistical analysis

The statistical analyses were performed using R (version 4.2.1). Variables are reported as mean (SD) unless otherwise stated. For all analyses, a p -value < 0.05 was considered statistically significant. MRI volumetric parameters are presented as a parenchymal fraction (PF), defined as the ratio of brain parenchymal volume to total intracranial volume unless otherwise stated.

DVR values of the prespecified ROIs were analyzed in HCs, all MS patients and in subgroups of RRMS and SPMS, as well as stratified by sex. Wilcoxon rank-sum test was used for group comparisons between categorical variables and DVRs. Multiple comparisons were corrected using a false discovery rate (FDR). Spearman correlation test was used to evaluate correlations of DVRs and EDSS. Reported p -values are naïve unless otherwise stated.

To adjust the results for confounding factors, a multiple linear regression model was used for patient data, and a linear mixed model with center as a random effect for controls, as they were from two different imaging centers. R software package lmerTest (version 3.1.3) was used for the mixed model. The used covariates were age, sex, brain volume (cm³) and body mass index (BMI). The model assumption was checked using Shapiro–Wilk's test (for normality of the residuals), variance inflation factors and Cook's distance (for influential observations), and, in case of influential observations, results were confirmed by analyzing the dataset without such observation.

Voxel-wise parametric binding potential (BP_{ND}) maps were calculated using basis function implementation of SRTM (29) with 250 basis functions. These were then converted into DVR (BP_{ND} + 1). Lower and upper bounds for theta were set to 0.06 1/min and 0.8 1/min. The resulting parametric maps were normalized to MNI space (Montreal Neurological Institute database) in SPM8. Mean PET images were obtained using the normalized parametric maps. The associations of radioligand binding and EDSS were evaluated with multiple regression model using normalized parametric binding potential images in MNI space. Analysis was performed for all MS patients, as well as for male and female patients separately. To ensure normality before the statistical analysis, the images were smoothed with 3D Gaussian 8 mm FWHM (full width at half maximum) filter. Multiple comparisons were corrected at the cluster level using the FWE (family-wise error) rate, and the critical significance level to reject the null hypothesis was set to 0.001.

3 Results

3.1 Demographic and clinical characteristics of study participants

The study cohort consisted of 102 MS patients with a mean (SD) age of 45.3 (9.7) years most of whom were females ($n = 73$, 72%). Median disease duration at the time of PET imaging was 12.1 [interquartile range (IQR) 7.0–17.2] years, and median EDSS 3.0 (IQR 2.0–3.9). No significant differences in age, disease duration, EDSS, annualized relapse rate (ARR) from disease onset to PET imaging, treatment, or BMI were observed between male and female patients at PET imaging (Table 1). All demographic information and MS-disease-related details are presented in Table 1.

3.2 Brain MRI outcomes of the study participants

Brain volume, NAWM, cortical GM (cGM) and thalamus volumes were larger among HCs compared to patients with MS (Table 2). As expected, SPMS patients had smaller brain volume as well as smaller NAWM and cGM volumes, but larger T1 and T2 lesion loads

TABLE 1 Demographic and clinical characteristics of the study cohort.

	HC	MS	HC vs. MS, <i>p</i> -value	RRMS	SPMS	RRMS vs. SPMS, <i>p</i> -value	Male MS	Female MS	Male vs. female MS, <i>p</i> -value
Subjects, <i>n</i>	76	102		75	27		29	73	
Female, <i>n</i> (%)	46 (61)	73 (72)	0.15	56 (75)	17 (63)	0.3	–	–	–
Age (years)	45.5 (14.5)	45.3 (9.7)	0.8	42.9 (8.9)	51.7 (9.2)	<0.001	45.9 (9.8)	45.0 (9.8)	0.9
BMI (kg/m ²)†	25.2 (4.0)	26.5 (5.8)	0.3	27.2 (5.8)	24.8 (5.8)	0.024	26.5 (5.3)	26.6 (6.1)	0.6
Disease duration (years), median (IQR)	–	12.1 (7.0–17.2)	–	9.6 (4.8–13.8)	19.2 (13.9–22.9)	<0.001	9.8 (3.2–16.9)	12.2 (7.7–17.3)	0.3
EDSS, median (IQR)	–	3.0 (2.0–3.9)	–	2.5 (2.0–3.0)	6.0 (4.25–6.5)	<0.001	3.0 (2.0–3.5)	3.0 (2.0–4.0)	0.9
ARR, median (IQR)	–	0.31 (0.22–0.53)	–	0.4 (0.2–0.6)	0.24 (0.18–0.40)	0.010	0.4 (0.2–0.6)	0.3 (0.2–0.5)	0.6
Disease modifying therapy, <i>n</i> (%)									
No therapy	–	48 (47)	–	25 (33)	23 (85)	< 0.001	14 (48)	34 (47)	0.3
Low-moderate efficacy	–	51 (50)	–	47 (63)	4 (15)		13 (45)	38 (52)	
High-efficacy	–	3 (3)	–	3 (4)	0 (0)		2 (7)	1 (1)	

Values are mean (SD) unless otherwise stated. For group comparisons, value of *ps* are from Wilcoxon rank-sum test. Significant *p*-values are bolded. Disease duration is years from first symptoms. Low-moderate efficacy therapy includes interferon beta, glatiramer acetate, dimethyl fumarate, teriflunomide and fingolimod. High-efficacy therapy includes natalizumab and rituximab. †BMI has one missing value in MS (female, RRMS) and two missing values in HC (male and female). ARR, annualized relapse rate; BMI, body mass index; EDSS, Expanded Disability Status Scale; HC, healthy control; MS, multiple sclerosis; RRMS, relapsing remitting MS; SPMS, secondary progressive MS.

compared to RRMS patients (Table 2). Among all the studied subgroups, i.e., all MS, HCs, RRMS and SPMS subjects, the total brain volume (cm³) was larger in males compared to females. When brain volume was normalized to the total intracranial volume (PF), healthy females had larger brain volume than female MS-patients, but no such difference was observed in males (Table 3). Of the subregions of interest, male RRMS patients had larger NAWM volumes compared to females. No differences in the T1 or T2 lesion loads between male and female RRMS patients was observed. Among SPMS patients, no differences in brain volumes between males and females were observed. The NAWM, cGM and thalamus volumes were larger among healthy females compared to female MS patients. Volumetric differences were less prominent between male patients and control males, where cGM and thalamus, but not NAWM, volumes were larger among HC males (Table 3).

3.3 TSPO radioligand binding in patients with MS vs. healthy controls and in RRMS vs. SPMS

[¹¹C](R)-PK11195 DVR values were higher in patients with MS compared to HCs in the whole brain [1.20 (0.03) vs. 1.19 (0.03), *p*=0.001], NAWM [1.22 (0.05) vs. 1.18 (0.05), *p*<0.001], thalamus [1.34 (0.08) vs. 1.31 (0.07), *p*=0.035] and cGM [1.23 (0.04) vs. 1.22 (0.05), *p*=0.038] (Figure 1). SPMS patients had a higher DVR in the NAWM compared to RRMS patients [1.26 (0.06) vs. 1.20 (0.05), *p*<0.001]. No difference in TSPO-binding in other ROIs was observed between SPMS patients and RRMS patients. RRMS patients and SPMS patients had higher DVRs in whole brain, NAWM and thalamus

compared to HCs. All significant results in whole brain and NAWM also survived the FDR correction, but not in the thalamus and cGM.

3.4 Association between TSPO radioligand binding and disability status in patients with MS

In all MS patients, a moderate correlation between NAWM DVR and EDSS and a weak correlation between thalamus DVR and EDSS was observed (*R*=0.42, *p*<0.001 and *R*=0.2, *p*=0.044; respectively) (Figure 2A). The strength of correlation between NAWM DVR and EDSS was higher among male patients compared to females (*R*=0.57 vs. *R*=0.39). Correlation between thalamus DVR and EDSS was observed only in male MS patients (Figures 2B,C). The association of TSPO-binding and EDSS was also evaluated using parametric binding potential images to demonstrate visually the brain areas with high TSPO-binding associated to EDSS. High TSPO-binding in subcortical WM, especially in frontal WM was associated with EDSS in both sexes. Furthermore, in male patients, high TSPO-binding in WM tract surrounding basal ganglia and thalamus was associated with EDSS (Figures 3A–C).

3.5 TSPO radioligand binding in males vs. females

The specific binding of [¹¹C](R)-PK11195 in the brain was increased in both MS patients and in healthy control males compared to females. Compared to female MS patients, male MS patients had a

TABLE 2 MRI volumetric parameters of healthy controls, all MS patients and RRMS- and SPMS-subgroups.

	HC	MS	HC vs. MS, <i>p</i> -value	RRMS	SPMS	RRMS versus SPMS
Brain volume (PF)	0.855 (0.036)	0.828 (0.046)	<0.001	0.834 (0.043)	0.810 (0.050)	0.034
NAWM volume (PF)	0.35 (0.025)	0.33 (0.036)	<0.001	0.33 (0.026)	0.32 (0.053)	0.035
Cortical GM volume (PF)	0.33 (0.022)	0.31 (0.025)	<0.001	0.32 (0.021)	0.30 (0.031)	0.003
Thalamus volume (PF)	0.011 (0.0011)	0.010 (0.0013)	<0.001	0.010 (0.0011)	0.010 (0.0017)	0.059
T1 lesion load (cm ³), median (IQR)	–	2.95 (1.28–8.58)	–	2.32 (1.11–4.17)	11.2 (6.95–23.2)	<0.001
T2 lesion load (cm ³), median (IQR)	–	6.01 (2.88–17.6)	–	4.14 (2.60–10.9)	18.5 (11.1–34.6)	<0.001

Values are mean (SD) unless otherwise stated. For group comparisons, *p*-values are from Wilcoxon rank-sum test. Significant *p*-values are bolded.

GM, gray matter; HC, healthy control; IQR, interquartile range; MS, multiple sclerosis; NAWM, normal-appearing white matter; PF, parenchymal fraction; RRMS, relapsing remitting MS; SPMS, secondary progressive MS.

higher DVR in the whole brain [1.22 (0.04) vs. 1.20 (0.02), $p=0.002$] and in the NAWM [1.24 (0.06) vs. 1.21 (0.05), $p=0.006$], thalamus [1.37 (0.08) vs. 1.32 (0.02), $p=0.008$] and cGM [1.25 (0.04) vs. 1.23 (0.04), $p=0.028$] (Figure 4A). Similarly, compared to healthy females, healthy males had a higher DVR in the whole brain [1.20 (0.03) vs. 1.18 (0.03), $p=0.002$], WM [1.20 (0.05) vs. 1.16 (0.04), $p=0.003$], and thalamus [1.34 (0.06) vs. 1.29 (0.07), $p=0.003$] but not in cGM [1.23 (0.04) vs. 1.21 (0.05), $p=0.14$] (Figure 4B).

When RRMS- and SPMS-subgroups were analyzed separately, we noticed that sex differences in [¹¹C](R)-PK11195 binding were more prominent among SPMS patients compared to RRMS. Among the RRMS patients, males had higher [¹¹C](R)-PK11195-binding in the whole brain [1.22 (0.04) vs. 1.20 (0.02), $p=0.031$] and cGM [1.25 (0.03) vs. 1.23 (0.04), $p=0.038$], but not in the NAWM [1.21 (0.04) vs. 1.20 (0.05), $p=0.17$] or thalamus [1.35 (0.07) vs. 1.32 (0.07), $p=0.12$] (Figure 4C). Within the SPMS-subgroup, males had similarly a higher DVR in the whole brain [1.23 (0.03) vs. 1.20 (0.03), $p=0.021$] but also in the NAWM [1.30 (0.05) vs. 1.24 (0.05), $p=0.003$] compared to females. No statistically significant difference in [¹¹C](R)-PK11195-binding was observed in the thalamus [1.41 (0.09) vs. 1.32 (0.10), $p=0.059$] or cGM [1.24 (0.06) vs. 1.22 (0.04), $p=0.5$] (Figure 4D).

Compared to healthy females, female MS patients had a higher DVR in the whole brain [1.20 (0.02) vs. 1.18 (0.03), $p<0.001$], NAWM [1.21 (0.05) vs. 1.16 (0.04), $p<0.001$] and thalamus [1.32 (0.08) vs. 1.29 (0.07), $p=0.034$] (Figure 5A) but not in cGM [1.23 (0.04) vs. 1.21 (0.05), $p=0.062$]. On the other hand, compared to healthy males, male MS patients had a higher DVR only in the NAWM [1.24 (0.06) vs. 1.20 (0.05), $p=0.004$]. No significant difference in TSPO-binding was observed in the whole brain [1.22 (0.04) vs. 1.20 (0.03), $p=0.070$], thalamus [1.37 (0.08) vs. 1.34 (0.06), $p=0.11$] or cGM [1.25 (0.04) vs. 1.23 (0.04), $p=0.12$] between male MS patients and HCs (Figure 5B).

Mean parametric PET-images demonstrating visually the differences in TSPO-binding in different subgroups of the study cohort are presented in Supplementary Presentation S1.

3.6 Adjustment of the [¹¹C](R)-PK11195-binding results for confounding factors

When age, BMI and brain volume were considered as confounding factors in multiple linear regression modeling, the differences in DVR values between female and male MS patients as well as in healthy

males and females remained statistically significant in the whole brain ($p=0.006$ in MS group and 0.03 in HC group), NAWM ($p<0.001$ in MS group and $p=0.006$ in HC group) and thalamus ($p=0.006$ in MS group and $p=0.007$ in HC group) (Table 4). Among RRMS- and SPMS-subgroups, only the sex difference in SPMS NAWM DVR ($p=0.004$) remained significant after adjusting for confounding factors. In addition, after adjusting for confounding factors, male SPMS patients had a higher DVR in the thalamus ($p=0.040$) compared to females, although initially, there was no sex difference in thalamic DVR in the SPMS-subgroup.

4 Discussion

We sought to uncover differences in MS brain pathology among males and females that might contribute to a greater male propensity for clinical disability progression. Using TSPO-PET-imaging, we found increased TSPO-binding in several regions of interest in male MS brain compared to female MS brain. Interestingly, in healthy controls, TSPO-binding was similarly more prominent among males compared to females. This suggests that the TSPO-binding cells possess a sex-driven inherent variability, which may predispose male MS patients to a greater likelihood of progressive disease. The same phenomenon may contribute to the higher male prevalence and incidence of other neurodegenerative diseases, such as Parkinson's disease and amyotrophic lateral sclerosis (30, 31). Hence, a better understanding of sex differences concerning microglia and macrophage responses may contribute to better prevention of progression, and more successful treatment outcomes.

In addition to evaluating TSPO-binding between males and females among MS patients and healthy controls, we also assessed variability in TSPO-binding among SPMS patients and RRMS patients according to sex. We found that among the entire cohort of MS patients and healthy controls, male SPMS patients had the highest TSPO availability, whereas healthy females had the lowest TSPO availability. This agrees with association of microglial activation with neurodegeneration (32), a feature most prominent among SPMS males.

Microglia are myeloid cells that reside in the CNS and comprise 5 to 10% of total cells in the brain, depending on the region examined (33). As non-neuronal cells, microglia originate from common myeloid precursor cells in the embryonic yolk sac early in ontogeny (34, 35). Microglia have a critical role during brain development and

TABLE 3 MRI volumetric parameters of the study cohort by gender.

	All MS patients			RRMS patients			SPMS patients			HCs			Males HC versus MS, <i>p</i> -value	Females HC versus MS, <i>p</i> -value
	Males	Females	<i>p</i> -value	Males	Females	<i>p</i> -value	Males	Females	<i>p</i> -value	Males	Females	<i>p</i> -value		
Brain volume (PF)	0.83 (0.06)	0.83 (0.04)	0.3	0.85 (0.05)	0.83 (0.04)	0.063	0.81 (0.06)	0.81 (0.04)	0.9	0.86 (0.03)	0.85 (0.04)	0.6	0.2	<0.001
Brain volume (cm ³)	1.228 (122)	1.113 (95)	<0.001	1.265 (120)	1.128 (92)	<0.001	1.157 (92)	1.062 (89)	0.027	1.233 (99)	1.118 (105)	<0.001	0.6	0.7
NAWM volume (PF)	0.33 (0.043)	0.33 (0.033)	0.5	0.35 (0.027)	0.33 (0.027)	0.030	0.31 (0.057)	0.32 (0.052)	0.3	0.35 (0.024)	0.35 (0.026)	0.17	0.051	0.003
Cortical GM volume (PF)	0.31 (0.030)	0.31 (0.022)	0.4	0.32 (0.025)	0.32 (0.019)	0.8	0.30 (0.037)	0.30 (0.027)	0.2	0.33 (0.018)	0.33 (0.024)	0.5	0.006	<0.001
Thalamus volume (PF)	0.010 (0.0013)	0.010 (0.0013)	0.3	0.010 (0.0010)	0.010 (0.0011)	0.9	0.009 (0.0013)	0.010 (0.0019)	0.3	0.0105 (0.0009)	0.0112 (0.0012)	0.015	0.041	<0.001
T1 lesion load (cm ³), median (IQR)	2.78 (1.39–11.2)	3.28 (1.17–8.20)	0.6	2.04 (1.28–2.84)	2.33 (0.79–5.02)	0.7	13.88 (8.27–20.7)	8.71 (4.57–25.0)	0.4	–	–	–	–	–
T2 lesion load (cm ³), median (IQR)	10.7 (3.62–16.5)	5.43 (2.67–17.8)	0.2	4.19 (3.32–11.04)	4.07 (2.34–10.8)	0.4	20.8 (15.3–40.9)	17.8 (7.64–33.4)	0.6	–	–	–	–	–

Values are mean (SD) unless otherwise stated. For group comparisons, value of *p*s are from Wilcoxon rank-sum test. Significant *p*-values are bolded.

GM, gray matter; IQR, interquartile range; MS, multiple sclerosis; NAWM, normal-appearing white matter; PF, parenchymal fraction; RRMS, relapsing remitting MS; SPMS, secondary progressive MS.

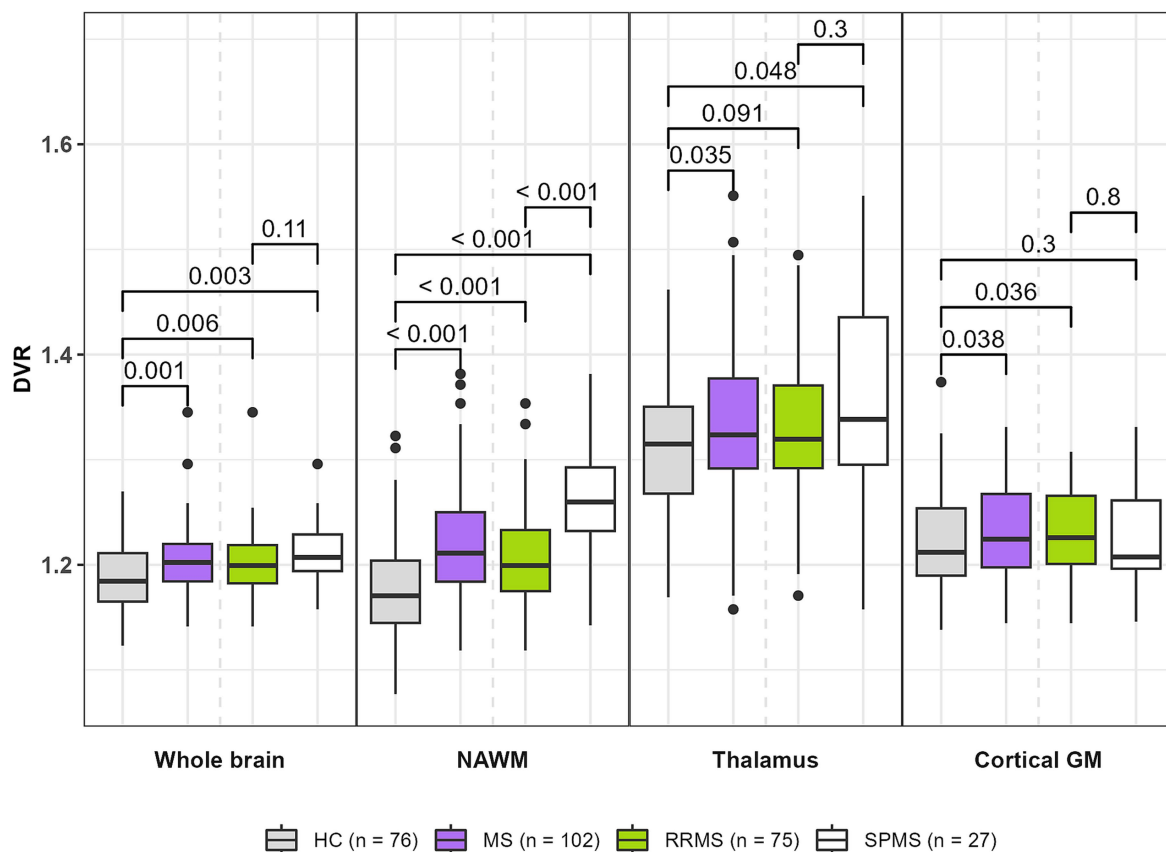


FIGURE 1

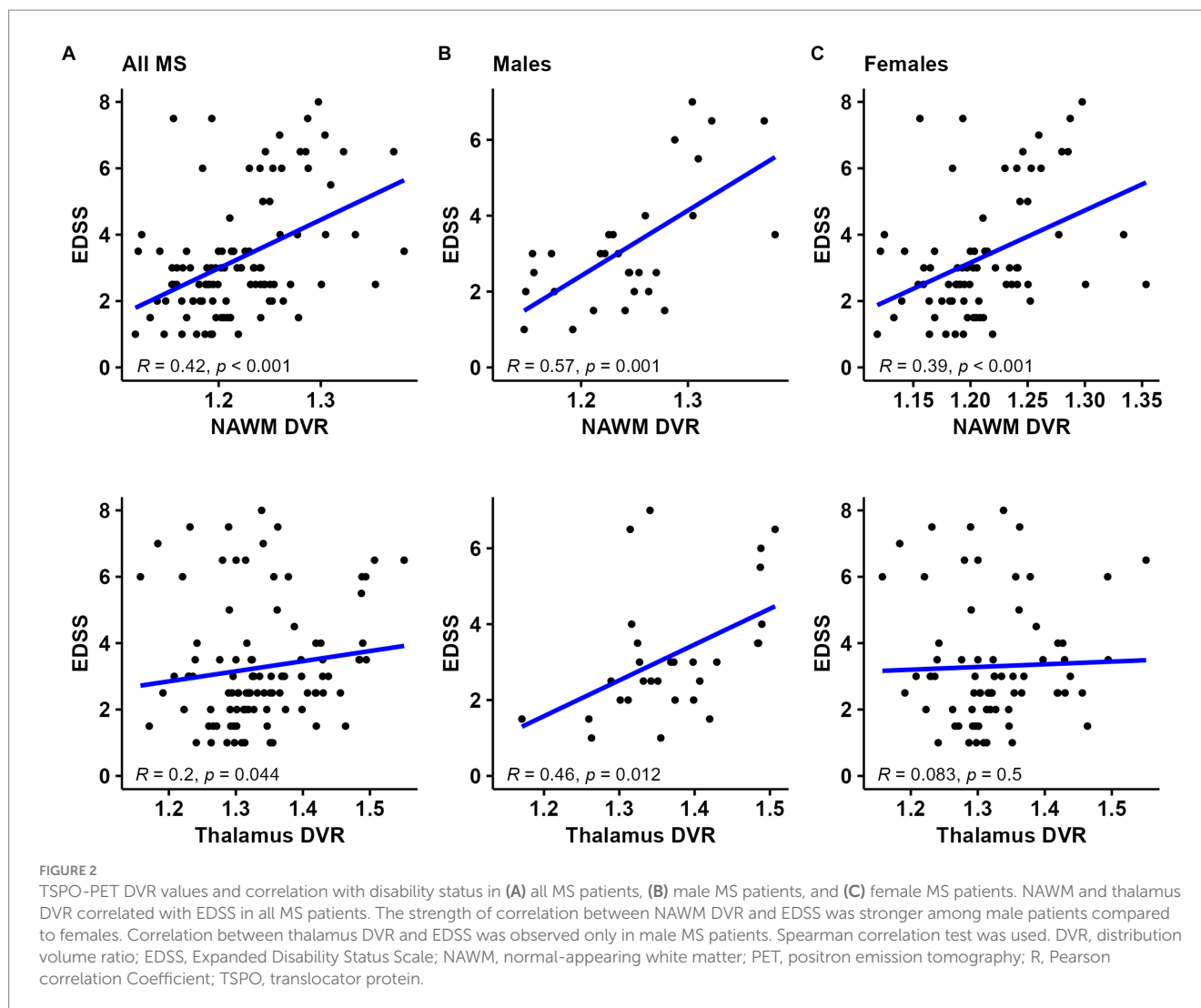
TSPO-PET DVR values in MS patients (all MS, RRMS, and SPMS) and healthy controls. MS patients had higher DVRs in whole brain, NAWM, thalamus and cortical GM compared to healthy controls. SPMS patients had a higher DVR in NAWM compared to RRMS patients. Compared to HCs, RRMS patients had higher DVRs in whole brain, NAWM and cortical GM. Compared to HCs, SPMS patients had higher DVRs in whole brain, NAWM and thalamus. Wilcoxon rank-sum test was used. All significant results in whole brain and NAWM also survived the FDR-correction, but not in thalamus and cortical GM. DVR, distribution volume ratio; GM, gray matter; HC, healthy control; MS, multiple sclerosis; NAWM, normal-appearing white matter; PET, positron emission tomography; RRMS, relapsing remitting MS; SPMS, secondary progressive MS; TSPO, translocator protein.

brain masculinization (35, 36). In mouse studies, the number and phenotype of microglia differ between males and females regionally, and in a time-specific manner (37, 38). There are mouse studies suggesting that adult microglia harbor several sex-biased features in their endogenous functions and responses to exogenous stimuli (39). Microglia from male mice express more genes associated with inflammatory processes, including regulation of cell migration and cytokine production, whereas female microglia express more genes linked to inhibition of inflammatory responses and promotion of repair mechanisms (40). Male microglia showed higher *in vitro* migration capacity than female microglia, both under basal and pro-inflammatory conditions, but female microglia had higher basal and pro-inflammatory stimulated phagocytic activity than male microglia (41).

Besides altered microglial phenotype, higher TSPO-binding may also signify higher microglial density (12). Microglial density in the brain is shown to be region dependent. For example, mouse studies have demonstrated significantly higher Iba1⁺ microglial cell density in the hippocampus, cortex, and amygdala in adult males compared to adult females (37). Microglia are long-lived cells which slowly renew throughout life (42). It is not presently known whether increased recruitment of microglial progenitor cells in early development or

more microglial proliferation and/or less microglial apoptosis throughout male life might explain the increased microglial density in males (36, 43). As with the previously discussed mouse studies, it is plausible that the higher TSPO availability in male MS and control brains reflects higher glial density in addition to altered phenotype among males compared to females. Interestingly, the TSPO molecule has been ascribed both proliferative and anti-apoptotic actions (44). To date, we are not aware of neuropathological studies in MS or in healthy individuals addressing this question. Given the sex differences in TSPO-binding in HCs, it is important to take this aspect into consideration with careful sex-matching of control cohorts in all future TSPO-PET and MRI studies addressing smoldering inflammation.

Differential signaling by steroid hormones may explain variations between male and female microglia as microglia express hormone receptors. Microglia from adult mouse brain express one or both estrogen receptor (ER) subtypes (ER α , ER β) (45, 46). In several studies, estrogen has shown to have an anti-inflammatory effect on microglia (47). Treatment of rat microglial cells with estrogen results in reduced lipopolysaccharide (LPS) -induced production of proinflammatory molecules such as inducible nitric oxide with reactive oxygen species production and prostaglandin E2 (48).



Selective estrogen-receptor modulators have been shown to suppress the production of proinflammatory cytokines and chemokines after LPS stimulation *in vitro* (49). Ovariectomy in rodents associates with changes in microglia morphology and accumulation of mRNA encoding inflammatory mediators (50). In the experimental autoimmune encephalomyelitis (EAE) estrogen alleviates EAE severity both in males and in females (51). The more pronounced TSPO-binding observed in our study among healthy men and male MS patients could possibly be explained by the more prominent protective role of estrogen in females.

Sex differences in microglial activation patterns following other brain injuries have been reported, but mostly using experimental animal models. In experimental stroke models, expression of pro-inflammatory markers by microglia were shown to be higher in males compared to females (52, 53). Microglia and infiltrating myeloid cells also have an important role in neuroinflammatory responses following traumatic brain injury (TBI). Male mice showed higher Iba-1-positive microglial density at the post-traumatic lesion border in the cortex (54), but the data regarding sex differences in TBI remain

somewhat conflicting (55, 56). A study addressing the sex difference in binding of a second generation TSPO-ligand, [¹¹C]PBR28, gave conflicting results regarding the above-described male predominance in TSPO-binding. Interestingly, this effect was abolished with aging (57). Altogether, limited number of studies investigating sex differences in TSPO radioligand binding are available and therefore further studies addressing this question are needed.

The sex difference in TSPO-binding described in this study extends to other myeloid cells, particularly macrophages. In a mouse obesity study, male macrophages were more inflammatory and more migratory compared to female macrophages, which had higher expression of anti-inflammatory cytokines (58). In another obesity study, male mice increased their myelopoiesis which enhanced the inflammatory phenomena in adipose tissue. In a competitive bone marrow transplant experiment, this took place irrespective of the hormonal status but was dependent on intrinsic sex differences in the myeloid cells (59). Similarly, in our cohort, we observed no statistically significant difference in TSPO-binding between pre- and post-menopausal women (data not shown), which together with the

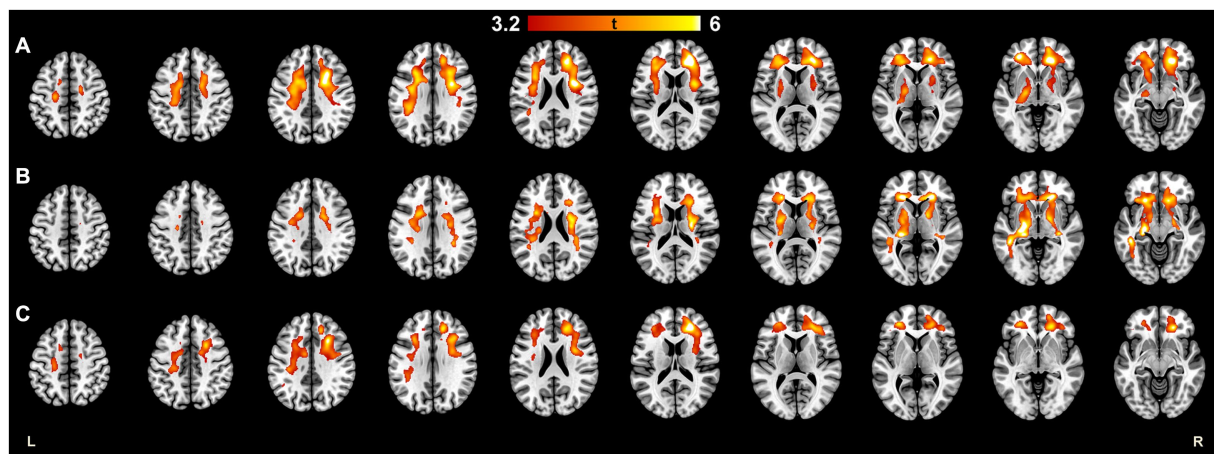


FIGURE 3

Statistical parametric mapping image demonstrating brain areas where the higher TSPO-radioligand binding was significantly associated with higher EDSS scores in (A) all MS patients, (B) male patients, and (C) female patients. High TSPO-binding in subcortical WM, especially in frontal WM was associated with EDSS in females and males. In male patients, high TSPO-binding in WM tract surrounding basal ganglia and thalamus was associated with EDSS. Multiple regression with EDSS as an explaining variable was performed using BPND images in MNI space. To ensure normality before the statistical analysis, the images were smoothed with 3D Gaussian 8 mm FWHM filter. Multiple comparisons were corrected using the FWE rate at cluster level, and the critical significance level to reject the null hypothesis was set to 0.001. The color scale of the marked areas refer to their t-statistic. BPND, normalized parametric binding potential; EDSS, Expanded disability status score; FWE, family-wise error; FWHM, full width at half maximum; HC, healthy control; MNI, Montreal Neurological Institute database; TSPO, translocator protein.

above-described rodent experiments suggests that the sex difference in TSPO binding might not be entirely driven by estrogens.

5 Conclusion

In conclusion, our work demonstrates for the first time increased TSPO-binding in several brain regions in males vs. females, both among people with MS and in healthy controls. This implies fundamental differences in innate immune cell phenotype and function between the sexes. Given the well-appreciated role of smoldering inflammation as a driver of MS progression, our work gives a plausible explanation for the increased risk of progression and neurodegeneration among men with MS.

Data availability statement

The raw data supporting the conclusions of this article will be made available by the authors, without undue reservation.

Ethics statement

The study was approved by Ethical committee of the Hospital District of Southwest Finland, Local Research Ethics Committee and Administration of Radioactive Substances Advisory Committee in the UK. The studies were conducted in accordance with the local legislation and institutional requirements. The participants provided their written informed consent to participate in this study.

Author contributions

SL: Conceptualization, Data curation, Investigation, Writing – original draft, Writing – review & editing. MS: Conceptualization, Writing – original draft, Writing – review & editing. MN: Investigation, Resources, Writing – review & editing. RH: Investigation, Resources, Writing – review & editing. AS: Investigation, Resources, Writing – review & editing. JR: Resources, Writing – review & editing. MM: Data curation, Formal analysis, Methodology, Writing – review & editing. LA: Conceptualization, Funding acquisition, Methodology, Supervision, Writing – original draft, Writing – review & editing.

Funding

The author(s) declare financial support was received for the research, authorship, and/or publication of this article. This work was funded by The Research Council of Finland grant for clinical researcher [330902]; Sigrid Juselius Foundation; The Research Council of Finland's Flagship In FLAMES [337530 and 357910] and Finnish Governmental Research Funding (VTR) grant for Turku University Hospital. The sponsors had no role in the design, execution, interpretation, or writing of the study.

Acknowledgments

We thank all subjects participating in this study, and the expert personnel of the Turku PET Centre for making this study possible. Jouni Tuisku from Turku PET Centre is acknowledged for his expert advice regarding the PET image processing.

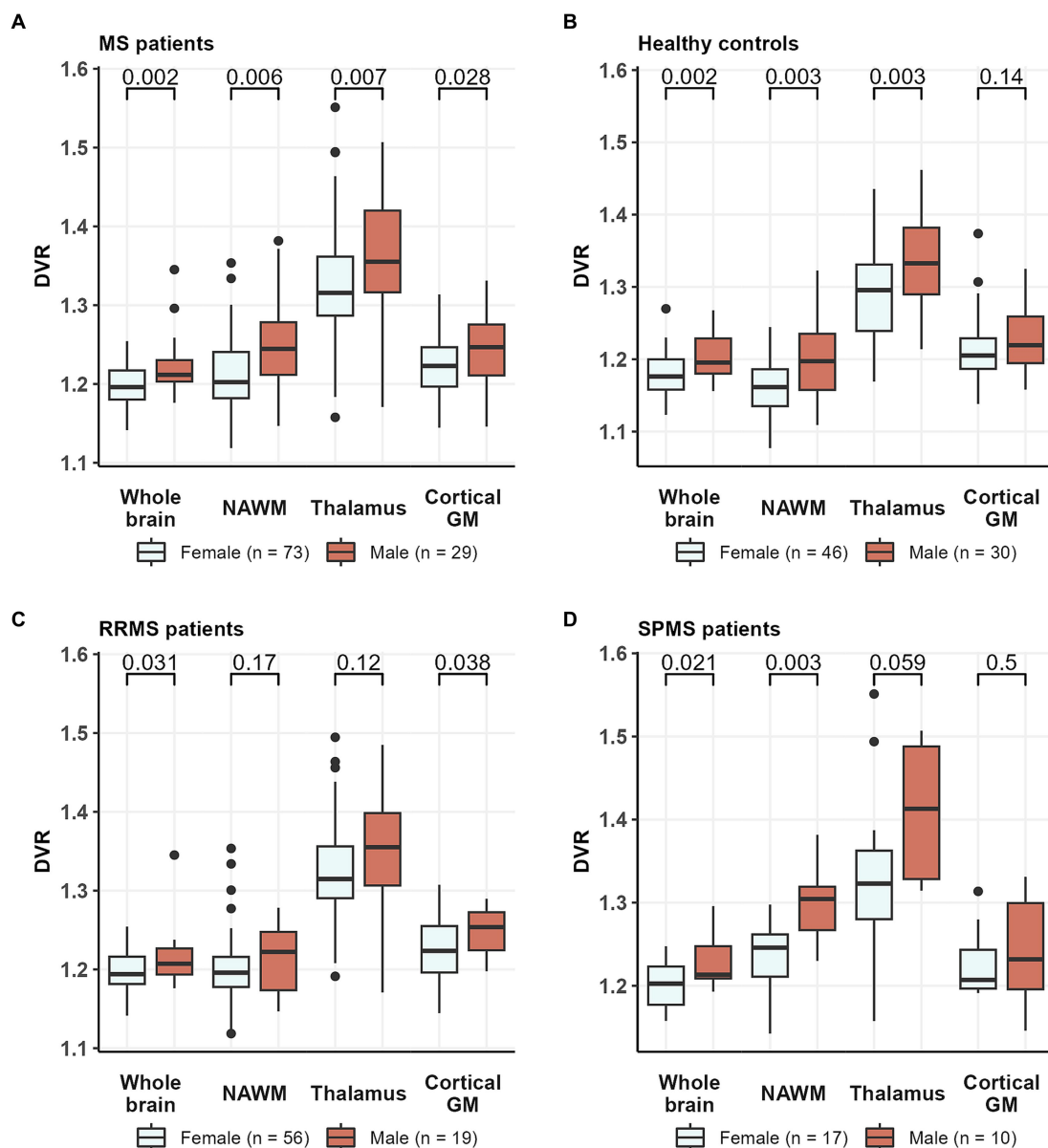


FIGURE 4

TSPO-PET DVR values in (A) all MS patients, (B) healthy controls, (C) RRMS patients, and (D) SPMS patients by sex. Male MS patients had a higher DVR in whole brain, NAWM, thalamus and cortical GM compared to female MS patients. Similarly, compared to healthy females, healthy males had a higher DVR in whole brain, NAWM and thalamus but not in cortical GM. Among RRMS patients, male patients had a higher DVR than females in whole brain and cortical GM, while in the SPMS group, male patients had a higher DVR than females in whole brain and NAWM. Wilcoxon rank-sum test was used. DVR, distribution volume ratio; MS, multiple sclerosis; NAWM, normal-appearing white matter; PET, positron emission tomography; RRMS, relapsing remitting multiple sclerosis; SPMS, secondary progressive multiple sclerosis; TSPO, translocator protein.

Conflict of interest

SL has received travel Honoria from Roche, and research support from the Turunmaa Duodecim society, Finnish Brain Foundation, Turku Doctoral Programme in Clinical Research and Finnish Governmental Research Funding (VTR) for Turku University Hospital. MN has received research support from the Finnish MS Foundation, Maire Taponen Foundation, the Finnish Cultural Foundation, Drug Research Doctoral Programme of University of Turku and the Research

Council of Finland's Flagship InFLAMES. AS was supported by the Emil Aaltonen foundation, the Paulo Foundation, the Orion Research Foundation sr, Finnish Governmental Research Funding (VTR) for Turku University Hospital and Research Council of Finland (#341059). JR serves as a neurology consultant for Clinical Research Services Turku (CSRT Oy). LA has received honoraria from Biogen, Roche, Genzyme, Merck Serono and Novartis, and institutional research grant support from the Research Council of Finland, Sanofi-Genzyme and Merck Serono.

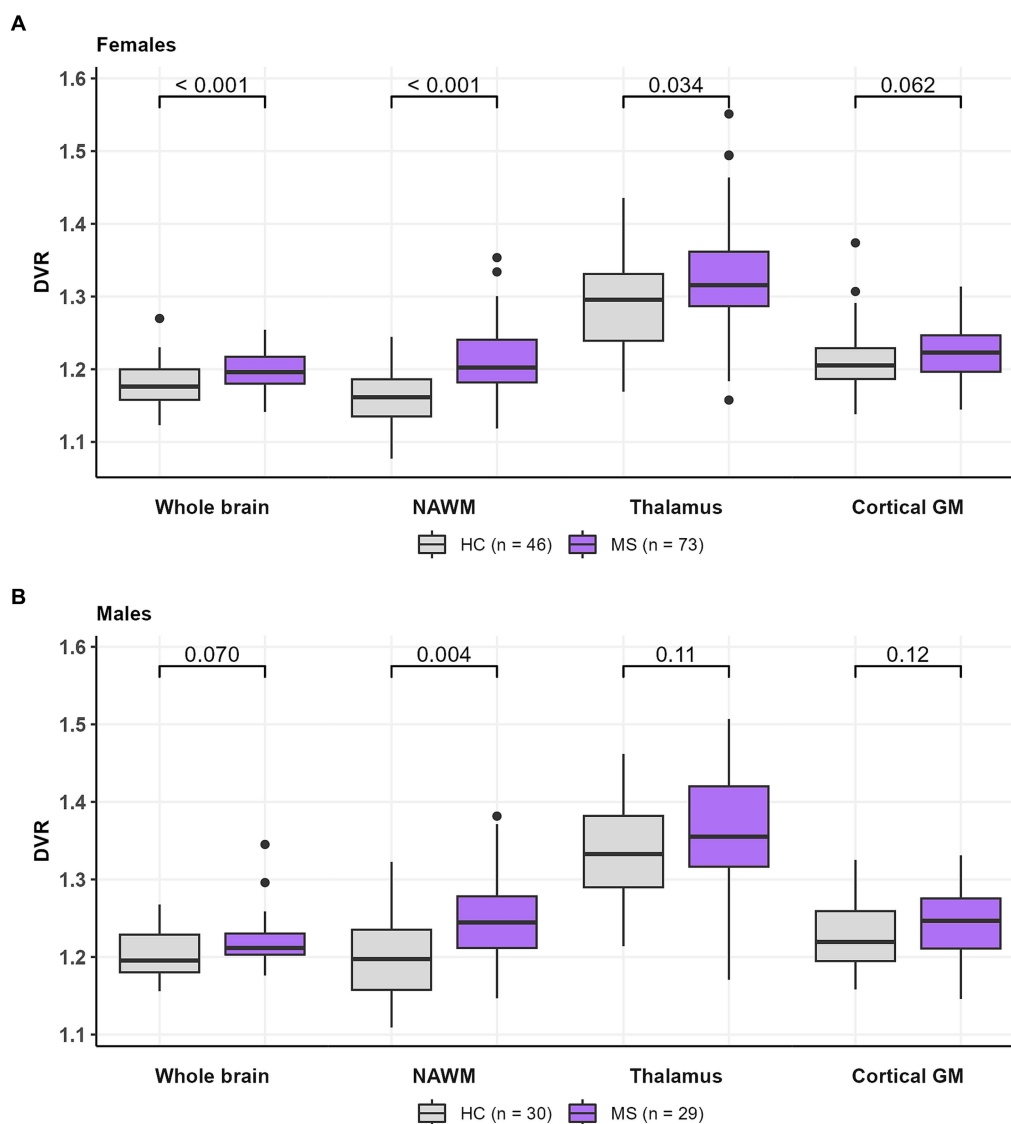


FIGURE 5

TSPO-PET DVR-values in (A) female HCs and MS patients and (B) male HCs and MS patients. Female MS patients had a higher DVR in whole brain, NAWM and thalamus compared to healthy females. Male MS patients had a higher DVR in NAWM compared to healthy males. No difference in DVR values in cortical GM between females and males were observed in HCs or MS patients. Wilcoxon rank-sum test was used. DVR, distribution volume ratio; HC, healthy control; MS, multiple sclerosis; NAWM, normal-appearing white matter; PET, positron emission tomography; TSPO, translocator protein.

The remaining authors declare that the research was conducted in the absence of any commercial or financial relationships that could be construed as a potential conflict of interest.

reviewers. Any product that may be evaluated in this article, or claim that may be made by its manufacturer, is not guaranteed or endorsed by the publisher.

Publisher's note

All claims expressed in this article are solely those of the authors and do not necessarily represent those of their affiliated organizations, or those of the publisher, the editors and the

Supplementary material

The Supplementary material for this article can be found online at: <https://www.frontiersin.org/articles/10.3389/fneur.2024.1352116/full#supplementary-material>

TABLE 4 Modeling the impact of sex and confounding factors on DVR in various brain regions in the studied cohorts.

Healthy controls (n = 76)					
Outcome DVR	Predictors	Estimate	95% CL		p-value
NAWM	Male vs. female	0.036	0.010	0.061	0.006
	Age	0.0008	-0.0001	0.0016	0.071
	Brain volume	0.0001	-0.0001	0.0002	0.3
	BMI	0.0001	-0.0025	0.0027	0.9
Whole brain	Male vs. female	0.018	0.002	0.033	0.030
	Age	0.0004	-0.0002	0.0009	0.19
	Brain volume	0.0000	0.0000	0.0001	0.2
	BMI	0.0018	0.0001	0.0034	0.042
Thalamus	Male vs. female	0.049	0.014	0.084	0.007
	Age	-0.0001	-0.0013	0.0010	0.8
	Brain volume	0.0000	-0.0001	0.0002	0.9
	BMI	-0.0024	-0.0061	0.0013	0.2
Cortical GM	Male vs. female	0.008	-0.017	0.033	0.5
	Age	0.0001	-0.0007	0.0010	0.8
	Brain volume	0.0000	-0.0001	0.0002	0.5
	BMI	0.0030	0.0003	0.0057	0.027

MS cohort (n = 102)					
Outcome DVR	Predictors	Estimate	95% CL		p-value
NAWM	Male vs. female	0.046	0.021	0.070	<0.001
	Age	0.0008	-0.0003	0.0018	0.17
	Brain volume	-0.0001	-0.0002	0.0000	0.047
	BMI	-0.0021	-0.0038	-0.0004	0.015
Whole brain	Male vs. female	0.020	0.006	0.034	0.006
	Age	0.0003	-0.0003	0.0009	0.3
	Brain volume	0.0000	0.0000	0.0001	0.6
	BMI	0.0007	-0.0002	0.0017	0.14
Thalamus	Male vs. female	0.055	0.016	0.094	0.006
	Age	-0.0005	-0.0022	0.0012	0.5
	Brain volume	-0.0001	-0.0002	0.0001	0.3
	BMI	-0.0027	-0.0053	0.0000	0.047
Cortical GM	Male vs. female	0.007	-0.012	0.026	0.4
	Age	0.0009	0.0000	0.0017	0.039
	Brain volume	0.0001	0.0000	0.0002	0.005
	BMI	0.0015	0.0001	0.0028	0.033

SPMS cohort (n = 27)					
Outcome DVR	Predictors	Estimate	95% CL		p-value
NAWM	Male vs. female	0.069	0.024	0.114	0.004
	Age	-0.0017	-0.0041	0.0007	0.15
	Brain volume	0.0000	-0.0003	0.0002	0.8
	BMI	0.0014	-0.0025	0.0053	0.5
Whole brain	Male vs. female	0.027	-0.001	0.054	0.058

(Continued)

TABLE 4 (Continued)

SPMS cohort (n = 27)					
Outcome DVR	Predictors	Estimate	95% CL		p-value
	Age	0.0003	-0.0012	0.0018	0.7
	Brain volume	0.0001	-0.0001	0.0002	0.4
	BMI	0.0015	-0.0008	0.0039	0.19
Thalamus	Male vs. female	0.087	0.004	0.169	0.040
	Age	-0.0045	-0.0089	-0.0001	0.046
	Brain volume	-0.0001	-0.0005	0.0003	0.6
	BMI	-0.0025	-0.0096	0.0046	0.5
Cortical GM	Male vs. female	0.008	-0.029	0.044	0.7
	Age	0.0016	-0.0003	0.0036	0.093
	Brain volume	0.0002	0.0000	0.0004	0.028
	BMI	0.0028	-0.0003	0.0059	0.078

RRMS cohort (n = 75)					
Outcome DVR	Predictors	Estimate	95% CL		p-value
NAWM	Male vs. female	0.021	-0.007	0.049	0.14
	Age	0.0005	-0.0007	0.0018	0.4
	Brain volume	-0.0001	-0.0002	0.0001	0.4
	BMI	-0.0017	-0.0035	0.0001	0.068
Whole brain	Male vs. female	0.014	-0.003	0.032	0.11
	Age	0.0001	-0.0007	0.0008	0.9
	Brain volume	0.0000	0.0000	0.0001	0.5
	BMI	0.0007	-0.0004	0.0019	0.2
Thalamus	Male vs. female	0.030	-0.014	0.075	0.18
	Age	0.0008	-0.0011	0.0028	0.4
	Brain volume	0.0000	-0.0002	0.0001	0.6
	BMI	-0.0013	-0.0042	0.0015	0.4
Cortical GM	Male vs. female	0.008	-0.015	0.031	0.5
	Age	0.0004	-0.0006	0.0015	0.4
	Brain volume	0.0001	0.0000	0.0002	0.054
	BMI	0.0010	-0.0006	0.0026	0.2

Modeling of the data was performed to explore the impact of sex with various confounding factors on DVR values in various brain regions in all studied cohorts. Results are based on linear mixed model (HCs) and multiple linear regression models (whole MS cohort and its subcohorts). Estimates with 95% confidence intervals and *p*-values for all predictors are presented in each model. In all other cohorts but in RRMS the impact of sex on TSPO-expressing microglia remained significant in most brain areas when confounding factors were considered. Significant *p*-values are bolded. The model assumption was checked and in case of an influential observations and results were confirmed by analyzing the dataset without such observation. This was the case in whole MS cohort with whole brain DVR as an outcome, in RRMS cohort with NAWM and whole brain DVRs as outcomes, and in SPMS cohort with cortical GM as an outcome. However, inferences regarding sex differences did not change. BMI, body mass index; CL, confidence interval; DVR, distribution volume ratio; GM, gray matter; HC, healthy control; MS, multiple sclerosis; NAWM, normal-appearing white matter; RRMS, relapsing–remitting MS; SPMS, secondary progressive MS.

References

- Voskuhl RR. The effect of sex on multiple sclerosis risk and disease progression. *Mult Scler.* (2020) 26:554–60. doi: 10.1177/1352458519892491
- Giovannoni G, Popescu V, Wuerfel J, Hellwig K, Iacobescu E, Jensen MB, et al. Smoldering multiple sclerosis: the ‘real MS’. *Ther Adv Neurol Disord.* (2022) 15:1–18. doi: 10.1177/17562864211066751
- Helmut K, Hanisch UK, Noda M, Verkhratsky A. Physiology of microglia. *Physiol Rev.* (2011) 91:461–553. doi: 10.1152/physrev.00011.2010
- Nutma E, Stephenson JA, Gorter RP, De Bruin J, Boucherie DM, Donat CK, et al. A quantitative neuropathological assessment of translocator protein expression in multiple sclerosis. *Brain.* (2019) 142:3440–55. doi: 10.1093/brain/awz287
- Yong VW. Microglia in multiple sclerosis: protectors turn destroyers. *Neuron.* (2022) 110:3534–48. doi: 10.1016/j.neuron.2022.06.023
- Muzio L, Viotti A, Martino G. Microglia in neuroinflammation and neurodegeneration: from understanding to therapy. *Front Neurosci.* (2021) 15:742065. doi: 10.3389/fnins.2021.742065
- Zrzavy T, Hametner S, Wimmer I, Butovsky O, Weiner HL, Lassmann H. Loss of “homeostatic” microglia and patterns of their activation in active multiple sclerosis. *Brain.* (2017) 140:1900–13. doi: 10.1093/brain/awx113
- Banati RB, Newcombe J, Gunn RN, Cagnin A, Turkheimer F, Heppner F, et al. The peripheral benzodiazepine binding site in the brain in multiple sclerosis. Quantitative

- in vivo imaging of microglia as a measure of disease activity. *Brain*. (2000) 123:2321–37. doi: 10.1093/brain/123.11.2321
9. Rissanen E, Tuisku J, Rokka J, Paavilainen T, Parkkola R, Rinne JO, et al. In vivo detection of diffuse inflammation in secondary progressive multiple sclerosis using PET imaging and the Radioligand 11C-PK11195. *J Nucl Med*. (2014) 55:939–44. doi: 10.2967/jnumed.113.131698
 10. Giannetti P, Politis M, Su P, Turkheimer FE, Malik O, Keihaninejad S, et al. Increased PK11195-PET binding in normal-appearing white matter in clinically isolated syndrome. *Brain*. (2015) 138:110–9. doi: 10.1093/brain/awu331
 11. Nutma E, Ceyzeriat K, Amor S, Tsartsalis S, Millet P, Owen DR, et al. Cellular sources of TSPO expression in healthy and diseased brain. *Eur J Nucl Med Mol Imaging*. (2021) 49:146–63. doi: 10.1007/s00259-020-05166-2
 12. Nutma E, Gebro E, Marzin MC, van der Valk P, Matthews PM, Owen DR, et al. Activated microglia do not increase 18 kDa translocator protein (TSPO) expression in the multiple sclerosis brain. *Glia*. (2021) 69:2447–58. doi: 10.1002/glia.24052
 13. Absinta M, Maric D, Gharagozloo M, Garton T, Smith MD, Jin J, et al. A lymphocyte–microglia–astrocyte axis in chronic active multiple sclerosis. *Nature*. (2021) 597:709–14. doi: 10.1038/S41586-021-03892-7
 14. Schirmer L, Velmsheshev D, Holmqvist S, Kaufmann M, Werneburg S, Jung D, et al. Neuronal vulnerability and multilineage diversity in multiple sclerosis. *Nature*. (2019) 573:75–82. doi: 10.1038/S41586-019-1404-Z
 15. Jäkel S, Agirre E, Mendanha Falcão A, van Bruggen D, Lee KW, Knuesel I, et al. Altered human oligodendrocyte heterogeneity in multiple sclerosis. *Nature*. (2019) 566:543–7. doi: 10.1038/S41586-019-0903-2
 16. Hamzaoui M, Garcia J, Boffa G, Lazzarotto A, Absinta M, Ricigliano VAG, et al. Positron emission tomography with [18 F]-DPA-714 unveils a smoldering component in most multiple sclerosis lesions which drives disease progression. *Ann Neurol*. (2023) 94:366–83. doi: 10.1002/ANA.26657
 17. Airas L, Yong VW. Microglia in multiple sclerosis - pathogenesis and imaging. *Curr Opin Neurol*. (2022) 35:299–306. doi: 10.1097/WCO.0000000000001045
 18. Rissanen E, Tuisku J, Vahlberg T, Sucksdorff M, Paavilainen T, Parkkola R, et al. Microglial activation, white matter tract damage, and disability in MS. *Neurol Neuroimmunol Neuroinflamm*. (2018) 5:e443. doi: 10.1212/nxi.0000000000000443
 19. Pitombeira MS, Koole M, Campanholo KR, Souza AM, Duran FLS, Solla DJF, et al. Innate immune cells and myelin profile in multiple sclerosis: a multi-tracer PET/MR study. *Eur J Nucl Med Mol Imaging*. (2022) 49:4551–66. doi: 10.1007/S00259-022-05899-2
 20. Saraste M, Matilainen M, Vuorimaa A, Laaksonen S, Sucksdorff M, Leppert D, et al. Association of serum neurofilament light with microglial activation in multiple sclerosis. *J Neurol Neurosurg Psychiatry*. (2023) 94:698–706. doi: 10.1136/JNPN-2023-331051
 21. Sucksdorff M, Matilainen M, Tuisku J, Polvinen E, Vuorimaa A, Rokka J, et al. Brain TSPO-PET predicts later disease progression independent of relapses in multiple sclerosis. *Brain*. (2020) 143:3318–30. doi: 10.1093/brain/awaa275
 22. Misin O, Matilainen M, Nylund M, Honkonen E, Rissanen E, Sucksdorff M, et al. Innate immune cell-related pathology in the thalamus signals a risk for disability progression in multiple sclerosis. *Neurol Neuroimmunol Neuroinflamm*. (2022) 9:e1182. doi: 10.1212/NXI.0000000000001182
 23. Koch M, Kingwell E, Rieckmann P, Tremlett HUBC MS Clinic Neurologists UMC. The natural history of secondary progressive multiple sclerosis. *J Neurol Neurosurg Psychiatry*. (2010) 81:1039–43. doi: 10.1136/jnnp.2010.208173
 24. Confavreux C, Vukusic S, Adeleine P. Early clinical predictors and progression of irreversible disability in multiple sclerosis: an amnesic process. *Brain*. (2003) 126:770–82. doi: 10.1093/brain/awg081
 25. Pozzilli C, Tomassini V, Marinelli F, Paolillo A, Gasperini C, Bastianello S. “Gender gap” in multiple sclerosis: magnetic resonance imaging evidence. *Eur J Neurol*. (2003) 10:95–7. doi: 10.1046/J.1468-1331.2003.00519.X
 26. Schoonheim MM, Popescu V, Lopes FCR, Wiebenga OT, Vrenken H, Douw L, et al. Subcortical atrophy and cognition: sex effects in multiple sclerosis. *Neurology*. (2012) 79:1754–61. doi: 10.1212/WNL.0b013e3182703f46
 27. RH BB, Zivadinov R, RH BB, Zivadinov R. Risk factors for and management of cognitive dysfunction in multiple sclerosis. *Nat Clin Pract Neurol*. (2011) 7:332–42. doi: 10.1038/NRNEUROL.2011.61
 28. Schmidt P, Gaser C, Arsic M, Buck D, Förtschler A, Berthele A, et al. An automated tool for detection of FLAIR-hyperintense white-matter lesions in multiple sclerosis. *NeuroImage*. (2012) 59:3774–83. doi: 10.1016/j.neuroimage.2011.11.032
 29. Gunn RN, Lammertsma AA, Hume SP, Cunningham VJ. Parametric imaging of ligand-receptor binding in PET using a simplified reference region model. *NeuroImage*. (1997) 6:279–87. doi: 10.1006/NIMG.1997.0303
 30. Erkkonen MG, Kim MO, Geschwind MD. Clinical neurology and epidemiology of the major neurodegenerative diseases. *Cold Spring Harb Perspect Biol*. (2018) 10:a033118. doi: 10.1101/CSHPERSPECT.A033118
 31. Longinetti E, Fang F. Epidemiology of amyotrophic lateral sclerosis: an update of recent literature. *Curr Opin Neurol*. (2019) 32:771–6. doi: 10.1097/WCO.0000000000000730
 32. Lassmann H. Pathogenic mechanisms associated with different clinical courses of multiple sclerosis. *Front Immunol*. (2018) 9:3116. doi: 10.3389/fimmu.2018.03116
 33. Lawson LJ, Perry VH, Dri P, Gordon S. Heterogeneity in the distribution and morphology of microglia in the normal adult mouse brain. *Neuroscience*. (1990) 39:151–70. doi: 10.1016/0306-4522(90)90229-W
 34. Alliot F, Godin I, Pessac B. Microglia derive from progenitors, originating from the yolk sac, and which proliferate in the brain. *Dev Brain Res*. (1999) 117:145–52. doi: 10.1016/S0165-3806(99)00113-3
 35. Nissen JC. Microglial function across the Spectrum of age and gender. *Int J Mol Sci*. (2017) 18:561. doi: 10.3390/IJMS18030561
 36. Lenz KM, McCarthy MM. A starring role for microglia in brain sex differences. *Neuroscientist*. (2015) 21:306–21. doi: 10.1177/1073858414536468
 37. Guneykaya D, Ivanov A, Hernandez DP, Haage V, Wojtas B, Meyer N, et al. Transcriptional and translational differences of microglia from male and female brains. *Cell Rep*. (2018) 24:2773–2783.e6. doi: 10.1016/J.CELREP.2018.08.001
 38. Schwarz JM, Sholar PW, Bilbo SD. Sex differences in microglial colonization of the developing rat brain. *J Neurochem*. (2012) 120:948–63. doi: 10.1111/J.1471-4159.2011.07630.X
 39. Han J, Fan Y, Zhou K, Blomgren K, Harris RA. Uncovering sex differences of rodent microglia. *J Neuroinflammation*. (2021) 18:74. doi: 10.1186/S12974-021-02124-Z
 40. Villa A, Gelos P, Castiglioni L, Cimino M, Rizzi N, Pepe G, et al. Sex-specific features of microglia from adult mice. *Cell Rep*. (2018) 23:3501–11. doi: 10.1016/J.CELREP.2018.05.048
 41. Yanguas-Casás N, Crespo-Castrillo A, de Ceballos ML, Chowen JA, Azcoitia I, Arevalo MA, et al. Sex differences in the phagocytic and migratory activity of microglia and their impairment by palmitic acid. *Glia*. (2018) 66:522–37. doi: 10.1002/GLIA.23263
 42. Réu P, Khosravi A, Bernard S, Mold JE, Salehpour M, Alkass K, et al. The lifespan and turnover of microglia in the human brain. *Cell Rep*. (2017) 20:779–84. doi: 10.1016/J.CELREP.2017.07.004
 43. Askew K, Li K, Olmos-Alonso A, Garcia-Moreno F, Liang Y, Richardson P, et al. Coupled proliferation and apoptosis maintain the rapid turnover of microglia in the adult brain. *Cell Rep*. (2017) 18:391–405. doi: 10.1016/J.CELREP.2016.12.041
 44. Veenman L, Papadopoulos V, Gavish M. Channel-like functions of the 18-kDa translocator protein (TSPO): regulation of apoptosis and steroidogenesis as part of the host-defense response. *Curr Pharm Des*. (2007) 13:2385–405. doi: 10.2174/138161207781368710
 45. Baker AE, Brautigam VM, Watters JJ. Estrogen modulates microglial inflammatory mediator production via interactions with estrogen receptor beta. *Endocrinology*. (2004) 145:5021–32. doi: 10.1210/EN.2004-0619
 46. Sierra A, Gottfried-Blackmore A, Milner TA, McEwen BS, Bulloch K. Steroid hormone receptor expression and function in microglia. *Glia*. (2008) 56:659–74. doi: 10.1002/GLIA.20644
 47. Villa A, Vegeto E, Poletti A, Maggi A. Estrogens, neuroinflammation, and neurodegeneration. *Endocr Rev*. (2016) 37:372–402. doi: 10.1210/er.2016-1007
 48. Vegeto E, Bonincontro C, Pollio G, Sala A, Viappiani S, Nardi F, et al. Estrogen prevents the lipopolysaccharide-induced inflammatory response in microglia. *J Neurosci*. (2001) 21:1809–18. doi: 10.1523/JNEUROSCI.21-06-01809.2001
 49. Ishihara Y, Itoh K, Ishida A, Yamazaki T. Selective estrogen-receptor modulators suppress microglial activation and neuronal cell death via an estrogen receptor-dependent pathway. *J Steroid Biochem Mol Biol*. (2015) 145:85–93. doi: 10.1016/J.JSBMB.2014.10.002
 50. Benedusi V, Meda C, Della Torre S, Monteleone G, Vegeto E, Maggi A. A lack of ovarian function increases neuroinflammation in aged mice. *Endocrinology*. (2012) 153:2777–88. doi: 10.1210/EN.2011-1925
 51. Spence RD, Voskuhl RR. Neuroprotective effects of estrogens and androgens in CNS inflammation and neurodegeneration. *Front Neuroendocrinol*. (2012) 33:105–15. doi: 10.1016/j.yfrne.2011.12.001
 52. Xiong X, Xu L, Wei L, White RE, Ouyang YB, Giffard RG. IL-4 is required for sex differences in vulnerability to focal ischemia in mice. *Stroke*. (2015) 46:2271–6. doi: 10.1161/STROKEAHA.115.008897
 53. Seifert HA, Benedek G, Liang J, Nguyen H, Kent G, Vandenbark AA, et al. Sex differences in regulatory cells in experimental stroke. *Cell Immunol*. (2017) 318:49–54. doi: 10.1016/J.CELLIMM.2017.06.003
 54. Acaz-Fonseca E, Duran JC, Carrero P, Garcia-Segura LM, Arevalo MA. Sex differences in glia reactivity after cortical brain injury. *Glia*. (2015) 63:1966–81. doi: 10.1002/GLIA.22867
 55. Villapol S, Loane DJ, Burns MP. Sexual dimorphism in the inflammatory response to traumatic brain injury. *Glia*. (2017) 65:1423–38. doi: 10.1002/glia.23171

56. Doran SJ, Ritzel RM, Glaser EP, Henry RJ, Faden AI, Loane DJ. Sex differences in acute Neuroinflammation after experimental traumatic brain injury are mediated by infiltrating myeloid cells. *J Neurotrauma*. (2019) 36:1040–53. doi: 10.1089/NEU.2018.6019
57. Tuisku J, Plavén-Sigraý P, Gaiser EC, Airas L, Al-Abdulrasul H, Brück A, et al. Effects of age, BMI and sex on the glial cell marker TSPO – a multicentre [11 C]PBR28 HRRT PET study. *Eur J Nucl Med Mol Imaging*. (2019) 46:2329–38. doi: 10.1007/S00259-019-04403-7
58. Chen K-HE, Lainez NM, Coss D. Sex differences in macrophage responses to obesity-mediated changes determine migratory and inflammatory traits. *J Immunol*. (2021) 206:141–53. doi: 10.4049/JIMMUNOL.2000490
59. Singer K, Maley N, Mergian T, Del Proposto J, Cho KW, Zamarron BF, et al. Differences in hematopoietic stem cells contribute to sexually dimorphic inflammatory responses to high fat diet-induced obesity. *J Biol Chem*. (2015) 290:13250–62. doi: 10.1074/JBC.M114.634568